Journal of Applied Spectroscopy, Vol. 81, No. 3, July, 2014 (Russian Original Vol. 81, No. 3, May–June, 2014)

EXPERIMENTAL STUDY OF SOFT *X*-RAY EMISSION FROM Pd-LIKE Xe PUMPED BY CAPILLARY DISCHARGE

Y. Zhao,[a*] M. Xu,[a] Y. Xie,[b] L. Li,[a] Sh. Jiang,[a] H. Cui,[a] and Q. Wang[a]

UDC 543.422.8

Under different pressures, the temporal evolution and spectra of soft X-ray emission from a capillary discharge xenon plasma were measured with an X-ray diode and spectrometer, respectively. Transition lines from Xe^{8+} to Xe^{11+} were clearly observed and showed up as small spikes in the temporal profile. Within the 5–20 nm wavelength region, the spectra originating from transitions in the Xe^{8+} to Xe^{11+} ion species were observed between 9 and 19 Pa. Among these spectral lines, the 16.47 nm line arises from the transition between the $4d^9 5p\ ^1P_1$ level and the ground level of Pd-like xenon (Xe^{8+}). The $4d^9 5p\ ^1P_1$ level is the lower level of the 41.8 nm laser transition of $4d^9 5d\ ^1S_0$–$4d^9 5p\ ^1P_1$. However, lasing output at 41.8 nm was not observed. According to our analysis, in order to realize the 41.8 nm lasing output, it is necessary to increase the electron temperature and the abundance of Pd-like Xe ions in the capillary discharge plasma.

Keywords: *capillary discharge, Pd-like Xe, soft X-ray.*

Introduction. Soft *X*-ray lasers pumped by capillary discharge have been demonstrated to be a promising scheme that meets practical requirements in applications [1]. Ever since the first demonstration of a discharge pumped table-top soft *X*-ray laser by J. J. Rocca in 1994, there have been realized Ne-like Ar 46.9 [2] and 69.8 nm [3], Ne-like S 60.8 nm [4], and Ne-like Cl 52.9 nm [5] soft *X*-ray lasers pumped by capillary discharge. The Ne-like Ar 46.9 nm soft *X*-ray laser was amplified in a highly saturated regime, and its average laser output pulse energy of 0.88 mJ and peak power of 0.6 MW were obtained at a repetition rate of 4 Hz [6]. Ne-like ions have a stable closed shell configuration, which is favorable to maintain the gain time of the laser.

Despite the early success of Ne-like Ar 46.9 nm soft *X*-ray laser, no soft *X*-ray laser with wavelength shorter than 46.9 nm has been realized by capillary discharge based on the electron collisional excitation scheme. A shorter wavelength laser has many advantages such as diagnostics of higher density plasmas, higher resolution metrology, and so on. Therefore, it is of significant importance to realize shorter wavelength lasers with the electron collisional excitation scheme in a capillary discharge plasma. Because of this, we are focusing on soft *X*-ray lasers at 41.8 nm in Pd-like Xe (Xe^{8+}), which have a stable closed shell configuration. Based on the collisionally pumped optical-field-ionization (OFI) scheme, many groups have obtained Pd-like Xe 41.8 nm amplification pumped by a femtosecond laser system [7–10]. The saturated amplification of Pd-like Xe 41.8 nm lasers has been realized with the OFI scheme [8]. Compared to the OFI scheme, the capillary discharge scheme has the advantage of longer plasma length, lower cost, and simpler operation. It is believed that a Pd-like Xe 41.8 nm soft *X*-ray laser can be achieved with higer energy, longer gain lifetime, better beam quality, longer gain length, and higher energy conversion efficiency.

In this paper, by discharging gaseous xenon in a capillary to Z-pinch the plasma, the emission of Pd-like Xe and its spectra characteristics were studied. These results provide valuable approach to realize Pd-like Xe $4d^9 5d\ ^1S_0$–$4d^9 5p\ ^1P_1$ 41.8 nm soft *X*-ray lasers pumped by a capillary discharge.

Experiment Setup. This experiment was conducted with the apparatus described in [11], in which Ne-like Ar 46.9 nm [11] and 69.8 nm [3] laser output pumped by a capillary discharge has been reported. The capillary is 3 mm in inner diameter and 35 cm in length. The equipment consists mainly of the power supplies of the prepulse and the main

*To whom correspondence should be addressed.

[a]Harbin Institute of Technology, Harbin, China; e-mail: zhaoyp3@hit.edu.cn; [b]Changchun Institute of Optics, Fine Mechanics and Physics, Chinese Academy of Sciences, Changchun, China. Abstract of article is published in Zhurnal Prikladnoi Spektroskopii, Vol. 81, No. 3, p. 483, May–June, 2014.

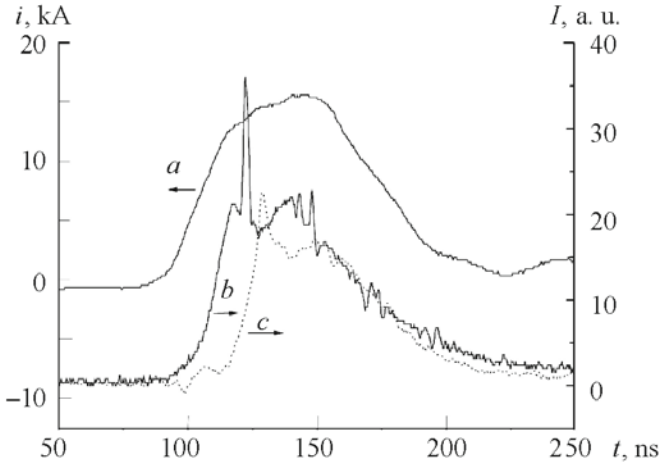

Fig. 1. Main current waveform (a) with amplitude 15 kA and temporal evolution of soft *X*-ray emission with Ar pressure 21 Pa (b) and Xe pressure 9 Pa (c).

pulse, vacuum and inflation system, discharge chamber, *X*-ray diode (XRD) detector, and associated control system. The capillary is continuously injected with xenon and differentially pumped by a turbo molecular pumped through a 1 mm diameter pinhole. The pressure in the capillary can be controlled by adjusting the flow control valve. The temporal evolution of soft *X*-ray emission was measured with the XRD, which can be replaced by a spectrometer to look at the spectra of soft *X*-ray emission from the capillary discharge xenon plasma. The spectra were measured with a 1 m grazing-incidence *X*-ray spectrograph (McPherson 248/310G) having a 600 lines/mm gold coated grating. The *X*-ray CCD (Andor Do420-BN-995) was used to record the time-integrated spectrum. The spectral range of the spectrograph is 6–100 nm, and its spectral resolution is 0.04 nm.

Prior to the fast discharge of the main current pulse, the xenon column in the capillary was preionized with a prepulse current of 20–25 A and 6 μs. The maximum voltage of the main pulse is 250 kV. The main current pulse, with a peak amplitude of 15 kA and rise-time of 30 ns, flowed through the preionized plasma column confined in a capillary tube. Then the plasma was strongly compressed and heated up in a Z-pinch-like behavior, which can generate a plasma column with a high length-to-diameter ratio of more than 1000:1. Such plasma produced by the fast Z-pinch is of high electron temperature and contains highly ionized species. These plasma properties are suitable for soft *X*-ray emission and for a soft *X*-ray laser. During the experiment, the device was operated at a repetition rate of 1 pulse per minute.

Results and Discussion. Firstly, under different initial Xe pressures, the temporal evolutions of soft *X*-ray emission from the capillary discharge xenon plasma were measured with the XRD. The amplitude of the main current pulse is 15 kA, and the initial pressure ranges from 8 to 90 Pa. A small spike with full width at half maximum (FWHM) of ~4 ns was observed in the temporal profile of the *X*-ray emission with gas pressure ranging from 8 to 10 Pa. The amplitude of the small spike reaches maximum at 9 Pa, as shown in Fig. 1c with its main current waveform (Fig. 1a). In other pressure ranges, no obvious spike was observed. To compare the spike of Xe plasma emission with the Ne-like Ar 46.9 nm laser spike, the temporal evolution of the Ar plasma was also measured at 21 Pa with the same current waveform as shown in Fig. 1b. The spike of Xe plasma emission is wider than the 46.9 nm laser spike (~2 ns) [11, 12] in pulse duration. Therefore, the spike of Xe plasma emission should be carefully studied to make certain whether it is a laser spike or not.

In order to verify the origin of the spike, the spectra of soft *X*-ray emission from the Xe plasma were measured and identified. With the same conditions as in Fig. 1, the time-integrated spectrum of soft *X*-ray emission was achieved and is shown in Fig. 2, which clearly presents very intense emission spectra near 13.5 nm. Note that there are no strong transition lines that were measured in the region 20–90 nm.

Based on the NIST atomic spectra database lines data [13] and [14], the observed transition lines were identified and labeled accordingly in Fig. 2. Table 1 lists the wavelengths with corresponding ion stages and transitions. The mismatches between observed wavelength and NIST wavelength are 0.01–0.06 nm. With the scope of the 0.04 nm spectral resolution of the spectrograph, the measured wavelengths agree well with the NIST wavelengths. From Fig. 2 and Table 1, the transition lines in the region 10–20 nm originate mainly from ions from Xe^{8+} to Xe^{11+}. The strong ~13.5 nm emission from

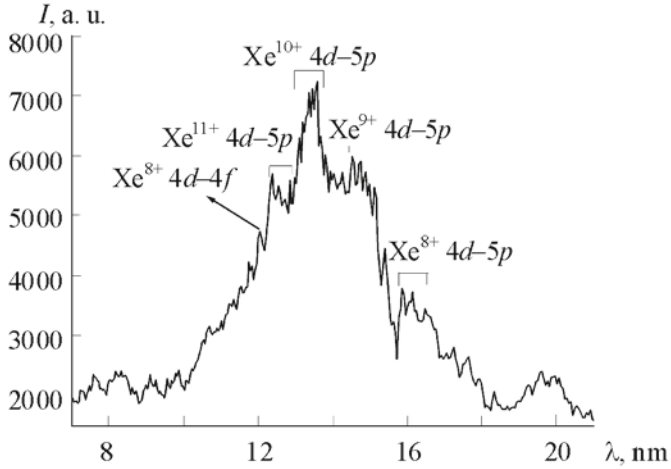

Fig. 2. Time-integrated spectrum of the axial emission from the Xe plasma column when the Xe pressure is 9 Pa, current 15 kA.

TABLE 1. Spectrum Identification of Soft *X*-ray Emission from Capillary Discharge Xenon Plasma

Ion stage	Transition	λ_{obs}, nm	λ_{NIST}, nm	Ion stage	Transition	λ_{obs}, nm	λ_{NIST}, nm
Xe^{6+}	$5s^2–4d^9 5s^2 4f$	15.39	15.383	Xe^{9+}	$4d^9–4d^8 5p$	14.88	14.9020
Xe^{8+}	$4d^{10}–4d^9 4f$	12.03	12.0133	Xe^{9+}	$4d^9–4d^8 5p$	14.98	15.0089
Xe^{8+}	$4d^{10}–4d^9 5p$	16.14	16.1742	Xe^{10+}	$4p^6 4d^8–4d^6 4d^7 5p$	13.36	13.3655
Xe^{8+}	$4d^{10}–4d^9 5p$	16.47	16.5323	Xe^{10+}	$4p^6 4d^8–4d^6 4d^7 5p$	13.45	13.4238
Xe^{9+}	$4d^9–4d^8 5p$	14.52	14.5150	Xe^{10+}	$4p^6 4d^8–4d^6 4d^7 5p$	13.58	13.5614
Xe^{9+}	$4d^9–4d^8 5p$	14.75	14.7618				

Xe^{10+} indicates that, in such discharge conditions, the Z-pinch generates a certain number of Xe^{10+} ions. Because there are no strong lines observed at 20–90 nm, the small spike of the XRD signal in Fig. 1 is not a laser signal but emission near 13.5 nm from Xe^{10+}. Based on the results of collisional-radiative (i.e., non-equilibrium) atomic-kinetic rate equations, we calculated the electron temperature to be 55 eV when the ~13.5 nm emission is strongest [15]. However, over-ionization of Xe^{8+} is a serious issue at this electron temperature, because the Xe^{9+} and Xe^{10+} were generated as shown in Fig. 2. Therefore the abundance of Xe^{8+} is low when the plasma was pinched to the axis.

The initial Xe pressure affects the output of the Pd-like Xe 41.8 nm laser due to the fact that the initial Xe pressure determines the abundance of Pd-like Xe in the final plasma column to some extent. In order to find the optimum pressure condition for Pd-like Xe production, the soft *X*-ray time-integrated spectra were studied in detail. Because the spectra observed in the 20–90 nm region are very weak, the spectra in the 7~21 nm region were investigated at 8.5~43 Pa with the discharge current corresponding to Fig. 1. Figure 3 shows some representative spectra. Looking at Figs. 2 and 3, one notes that increasing the pressure from 9 to19 Pa decreases the intensity of the ~13.5 nm emission from Xe^{10+} to a great extent. This decrease is much greater than the intensity decrease of the ~16 nm emission from Pd-like Xe. Increasing the pressure from 19 to 22 Pa we see that the intensity of the ~16 nm emission from Pd-like Xe exceeds the intensity of the ~13.5 nm emission from Xe^{10+}. The intensity of the ~16 nm emission is the strongest in the 7~21 nm range at 24 Pa. Because the spectrum of Xe^{9+} and Xe^{10+} is weak, the over-ionization of Pd-like Xe is not severe at 24 Pa, when the plasma is Z-pinched to the axis. With identical discharge current waveform, as the initial xenon pressure increases, the Xe atom density increases. Due to the increase in the mass per unit volume, the Z-pinch velocity and the energy of particle collisions both decrease, resulting in a decrease in the electron temperature. Under the same conditions, the decrease in electron temperature will reduce the density of Xe^{9+} and Xe^{10+} and lower the emission intensity from Xe^{9+} and Xe^{10+}, as shown in Fig. 3.

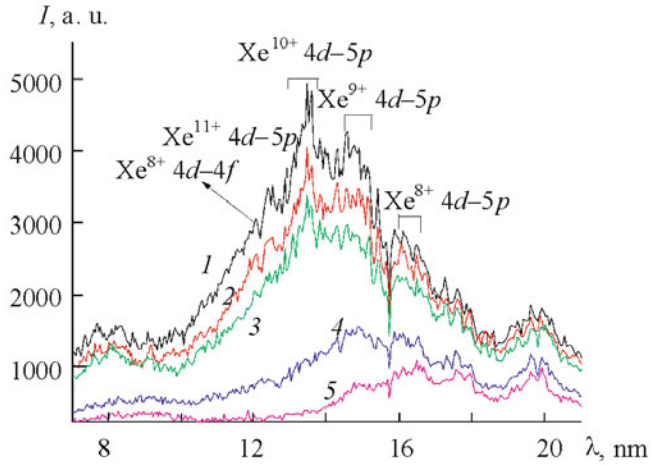

Fig. 3. Comparison of time-integrated spectra under different pressures when the main current amplitude is fixed at 15 kA, pressure 14 (1), 16 (2), 19 (3), 22 (4), and 24 Pa (5).

TABLE 2. Calculation Results on the Transitions in the Pd-Like Xe System

Transition	log F	A_s, s^{-1}	ΔE, eV	λ, nm
$4d^9 5d\ ^1S_0$–$4d^9 5f\ ^1P_1$	–0.022	$2.418 \cdot 10^{10}$	24.3	51.12
$4d^9 5d\ ^1P_1$–$4d^{99} 5f\ ^1P_1$	–0.440	$1.499 \cdot 10^{10}$	30.9	40.20
$4d^{10}\ ^1S_0$–$4d^9 5f\ ^1P_1$	0.247	$1.277 \cdot 10^{12}$	129.4	9.60
$4d^9 5d\ ^1S_0$–$4d^9 4f\ ^1P_1$	–1.181	$2.116 \cdot 10^{7}$	2.7	460.08
$4d^9 5d\ ^1S_0$–$4d^9 5p\ ^1P_1$	–0.164	$2.615 \cdot 10^{10}$	29.7	41.82
$4d^9 5d\ ^1P_1$–$4d^9 5p\ ^1P_1$	–0.075	$1.934 \cdot 10^{10}$	23.1	53.78
$4d^{10}\ ^1S_0$–$4d^9 5p\ ^1P_1$	0.041	$2.701 \cdot 10^{11}$	75.4	16.47

In order to observe the Xe^{8+} $4d^9 5d\ ^1S_0$–$4d^9 5p\ ^1P_1$ 41.8 nm transition line, we adjusted the spectrometer central wavelength to 46.9 nm. Because the spectra from Xe^{9+} and Xe^{10+} ions are weak at 24 Pa, as shown in Fig. 3, the over-ionization of Pd-like Xe is not a big concern. At a pressure of 24 Pa, the 41.8 nm transition line was not observed. However, when the Xe pressure is lowered to 14 Pa, at which the abundance of Xe^{10+} is high, the 41.8 nm transition line was detected, which is shown in Fig. 4. In order to identify the 41.8 nm line from the background, the spectrum between 40 and 50 nm was measured 10 times. The results show that the spectral lines at 41.8 and 42.0 nm can be observed every time. Some weaker spectral lines, which appear randomly, should originate from the overlapping fluctuations of continuous radiation. We believe that the reasons for the observation of the 41.8 nm line at 14 Pa are that although the over-ionization of Xe^{8+} is not as severe at lower pressures, and the electron temperature of the plasma is higher than at higher pressures.

To analyze the result of Fig. 4 and the 41.8 nm laser transition of the Pd-like Xe, the Xe^{8+} energy level parameters were calculated with the Cowan code, which is freely available on the Internet. Table 2 shows the results of partial-transition oscillator strengths (F), spontaneous emission rates (A_s), energy-level differences (ΔE), and transition wavelengths (λ). According to the calculation results and [7, 16], the partial energy level diagram related to Xe^{8+} $4d^9 5d\ ^1S_0$–$4d^9 5p\ ^1P_1$ 41.8 nm laser transitions is shown in Fig. 5. The Pd-like Xe at the ground level $4d^{10}\ ^1S_0$ is pumped to the upper level (metastable state) $4d^9 5d\ ^1S_0$ through electron collisional excitation, particularly monopole electron excitation. Because the transition from the lower level $4d^9 5p\ ^1P_1$ to the ground level is a dipole-allowable transition, its spontaneous radiation decay rate is very large ($2.701 \cdot 10^{11}$ s^{-1}). The fast radiation decay is favorable to the population inversion between upper and lower levels. When the Pd-like Xe on the upper level transits to the lower level, 41.8 nm line is emitted.

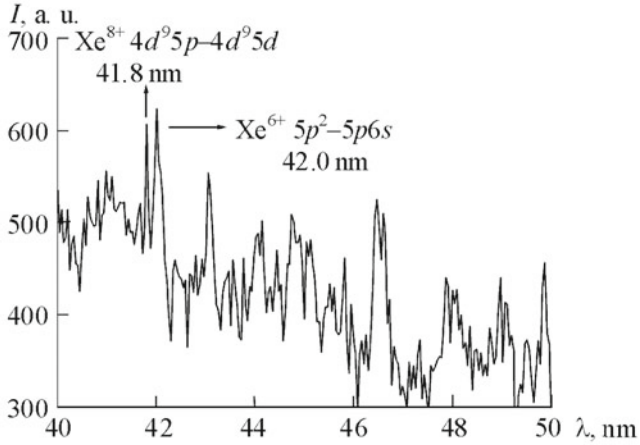

Fig. 4. The Xe^{8+} $4d^9 5d\ ^1S_0$–$4d^9 5p\ ^1P_1$ 41.8 nm transition line observed in the experiment, pressure 14 Pa, current 15 kA.

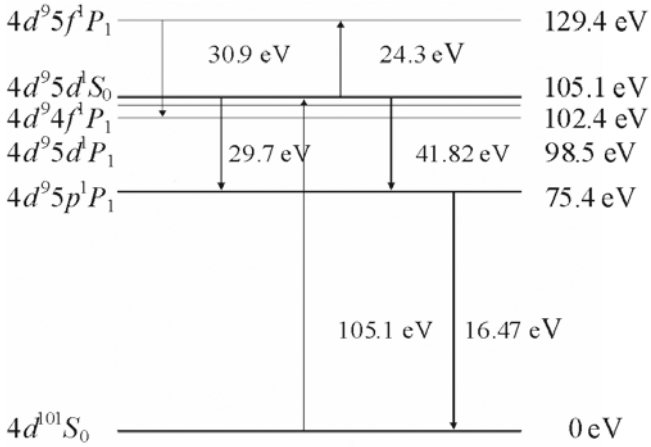

Fig. 5. Partial energy level diagram of the Xe^{8+} $4d^9 5d\ ^1S_0$–$4d^9 5p\ ^1P_1$ 41.8 nm laser transition.

The experimental results show that the Pd-like Xe 41.8 nm transition line is weak. However, the 16.47 nm transition line between the laser lower level $4d^9 5p\ ^1P_1$ and the ground level $4d^{10}\ ^1S_0$ is relatively intense, as illustrated in Fig. 3. These results indicate that the laser lower level is excited more effectively than the upper level. According to the calculation results in [17], in the OFI scheme the plasma realized 41.8 nm laser nonsaturated amplification [7] with $n_e = 3.4 \cdot 10^{24}$ m^{-3} and $T_e = 75$–100 eV. In addition, the plasma can also reach 41.8 nm laser saturated amplification [8] with $n_e = 4.8 \cdot 10^{24}$ m^{-3} and $T_e = 140$ eV. Because the strong ~13.5 nm emission band was observed at 9–19 Pa in our experiment, the electron temperature in the Xe plasma column should be about 55 eV [15]. The electron energy is too low to effectively excite the ground Pd-like Xe to the upper level of the 41.8 nm laser.

The OFI scheme can obtain a large abundance of Pd-like Xe through controlling pump laser intensity, and achieve optimum electron temperature by controlling pump laser polarization. Consequently it is easy to control the plasma state precisely. By contrast, in the capillary discharge scheme, it is difficult to control the plasma state exactly. The Z-pinch process of plasma can be controlled by adjusting the experimental parameters, such as capillary diameter, initial pressure, amplitude, and rise-time of main current, and so on. However, all these parameters cannot exactly determine the final state of the plasma column after the Z-pinch. Pd-like Xe 41.8 nm laser amplification requires a plasma column with high abundance of Pd-like

Xe and optimum electron temperature simultaneously. Our results tend to show that, in the present discharge conditions, a plasma column suitable for achieving Pd-like Xe 41.8 nm lasing cannot be achieved.

Conclusions. Theoretically, some energy level parameters were calculated and the partial energy level diagram of the Xe^{8+} $4d^9 5d\ ^1S_0$–$4d^9 5p\ ^1P_1$ 41.8 nm laser transition is given. Experimentally, the temporal evolution and time-integrated spectra of soft x-ray emission from a capillary discharge xenon plasma were investigated. In the Pd-like Xe 41.8 nm laser system, the transition line 16.47 nm from the lower level to the ground state is intense in the pressure range 9–19 Pa, and the weak 41.8 nm transition line was only observed at 14 Pa. The experimental results were analyzed based on the calculation results on partial energy levels. According to the analysis, in order to achieve 41.8 nm lasing, it is essential to improve the plasma electron temperature in the capillary. In the future we will increase the amplitude and decrease the rise-time of the main current pulse to ultimately improve the electron temperature through the quick Z-pinch before the Pd-like Xe reaches the over-ionization state.

Acknowledgments. This project is supported by the Research Fund for the Doctoral Program of Higher Education (No. 20102302110025) and National Natural Science Foundation of China (No. 61275139).

REFERENCES

1. J. J. Rocca, J. Filevich, E. C. Hammarsten, E. Jankowska, B. Benware, M. C. Marconi, B. Luther, A. Vinogradov, I. Artiukov, S. Moon, and V. N. Shlyaptsev, *Nucl. Instrum. Methods Phys. Res. A*, **507**, 515–522 (2003).
2. J. J. Rocca, V. Shlyaptsev, F. G. Tomasel, O. D. Cortazar, D. Hartshorn, and J. L. A. Chilla, *Phys. Rev. Lett*., **73**, 2192–2195 (1994).
3. Y. Zhao, S. Jiang, Y. Xie, D. Yang, S. Teng, D. Chen, and Q. Wang, *Opt. Lett.*, **36**, 3458–3460 (2011).
4. F. G. Tomasel, J. J. Rocca, V. N. Shlyaptsev, and C. D. Macchietto, *Phys. Rev. A*, **55**, 1437–1440 (1997).
5. M. Frati, M. Seminario, and J. J. Rocca, *Opt. Lett.*, **25**, 1022–1024 (2000).
6. C. D. Macchietto, B. R. Benware, and J. J. Rocca, *Opt. Lett.*, **24**, 1115–1117 (1999).
7. B. E. Lemoff, G. Y. Yin, C. L. Gordan III, C. P. J. Barty, and S. E. Harris, *Phys. Rev. Lett.*, **74**, 1574–1577 (1995).
8. S. Sebban, R. Haroutnian, Ph. Balcou, G. Grillon, A. Rousse, S. Kazamias, T. Marin, J. P. Rousseau, L. Notebaert, M. Pittman, J. P. Chambaret, A. Antonetti, D. Hulin, D. Ros, A. Klisnick, and A. Carillon, *Phys. Rev. Lett.*, **86**, 3004–3007 (2001).
9. A. Butler, A. J. Gonsalves, C. M. McKenna, D. J. Spence, S. M. Hooker, S. Sebban, T. Moccek, I. Bettaibi, and B. Cros, *Phys. Rev. Lett*., **91**, 205001 (2003).
10. H. H. Chu, H.-E. Tsai, M.-C. Chou, L.-S Yang, J.-Y. Lin, C.-H. Lee, J. Wang, and S.-Y. Chene, *Phys. Rev. A*, **71**, 061804 (2005).
11. Y. Zhao, Y. Cheng, B. Luan, Y. Wu, and Q. Wang, *J. Phys. D: Appl. Phys.*, **39**, 342–346 (2006).
12. Y. P. Zhao, Y. Xie, Q. Wang, and T. Liu, *Eur. Phys. J. D*, **49**, 379–382 (2008).
13. http://physics.nist.gov/PhysRefData/ASD/lines_form.html
14. M. A. Klosner and W. T. Silfvast, *J. Opt. Soc. Am. B*, **17**, 1279–1290 (2000).
15. B. S. Bauer, R. C. Mancini, V. Makhin, I. Paraschiv, A. Esaulov, and R. Presura, *Proc. SPIE*, **5374**, 394–404 (2004).
16. B. E. Lemoff, C. P. Barty, and S. E. Harris, *Opt. Lett.*, **19**, 569–571 (1994).
17. E. P. Ivanova, *Phys. Rev. A*, **84**, 043829 (2011).